

# Reduced Complexity Compression Algorithms for Direct-Write Maskless Lithography Systems

Hsin-I Liu, Vito Dai, Avideh Zakhor, and Borivoje Nikolić

Department of Electrical Engineering and Computer Science

University of California, Berkeley

{hsil, vdai, avz, bora}@eecs.berkeley.edu

## ABSTRACT

Achieving the throughput of one wafer layer per minute with a direct-write maskless lithography system, using 22 nm pixels for 45 nm feature sizes, requires data rates of about 12 Tb/s. In our previous work, we developed a novel lossless compression technique specifically tailored to flattened, rasterized, layout data called *Context-Copy-Combinatorial-Code (C4)* which exceeds the compression efficiency of all other existing techniques including BZIP2, 2D-LZ, and LZ77, especially under limited decoder buffer size, as required for hardware implementation. In this paper, we present two variations of the C4 algorithm. The first variation, Block C4, lowers the encoding time of C4 by several orders of magnitude, concurrently with lowering the decoder complexity. The second variation which involves replacing hierarchical combinatorial coding part of C4 with Golomb run-length coding, significantly reduces the decoder power and area as compared to Block C4. We refer to this algorithm as *Block Golomb Context Copy Code (Block GC3)*. We present the detailed functional block diagrams of Block C4 and Block GC3 decoders along with their hardware performance estimates as the first step of implementing the writer chip for maskless lithography.

**Keywords:** maskless lithography, complexity, implementation, decoder, prediction, buffer, memory, segmentation

## 1. INTRODUCTION

Future lithography systems must produce chips with smaller feature sizes, while maintaining throughput comparable to today's optical lithography systems. This places stringent data handling requirements on the design of any direct-write maskless system. Optical projection systems use a mask to project the entire chip pattern in one flash. An entire wafer can then be written in a few hundreds of such flashes. To be competitive with today's optical lithography systems, direct-write maskless lithography needs to achieve throughput of one wafer layer per minute. In addition for 45 nm technology, to achieve the 1nm edge placement required to comply with the minimum grid size specification as well as the 22 nm pixel size as the design rule scale, a 5-bit per pixel data representation is needed to refine the edge placement precision of pixels to less than 1 nm. Combining these together, the data rate requirement for a maskless lithography system is<sup>5,12</sup>

$$\frac{(300 \text{ mm})^2}{(22 \text{ nm})^2} \times \frac{\pi}{4} \times \frac{5 \text{ bits}}{60 \text{ s}} = 12 \text{ Tb/s}.$$

To achieve such a data rate, we have recently proposed<sup>5</sup> a data path architecture shown in Figure 1. In this architecture, rasterized, flattened layouts of an integrated circuit (IC) are compressed and stored in a mass storage system. Assuming a 10:1 compression ratio for all layers, the layout of a 22 mm × 22 mm chip with 40 layers occupies 20 Tb, as illustrated in Fig 1. The compressed layouts are then transferred to the processor board with enough memory to store one layer at a time. This board will transfer the compressed layout to the writer chip, composed of a large number of decoders and actual writing elements. The outputs of the decoders correspond to uncompressed layout data and are fed into D/A converters driving the writing elements such as a micromirror array or E-beam writers.

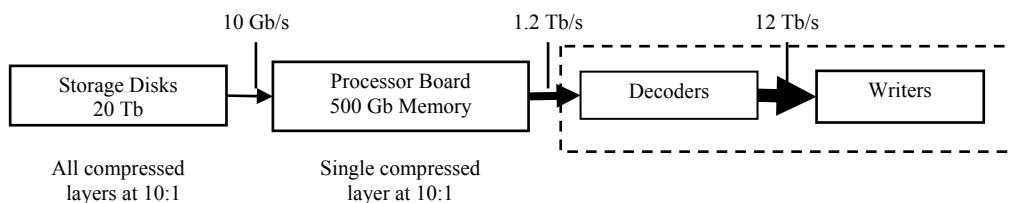


Figure 1. The data delivery path of maskless lithography.

In the proposed data-delivery path, compression is needed to minimize the transfer rate between the processor board and the writer chip, and also to minimize the required disk space to store the layout. In Figure 1, the total writer data rate of

12 Tb/s is reduced to 1.2 Tb/s assuming compression ratio of 10:1, and then further reduced to 10 Gb/s by using on-board memory with high performance I/O interfaces<sup>6</sup>. Since there are a large number of decoders operating in parallel on the writer chip, an important requirement for any compression algorithm is to have a very low decoder complexity. To this end, we have proposed a lossless layout compression algorithm for flattened, rasterized data called Context-Copy-Combinatorial-Code (C4) which has been shown to outperform all existing techniques such as BZIP2, 2D-LZ, and LZ77 in terms of compression efficiency, especially under limited decoder buffer size, as required for hardware implementation. However, a major drawback of the C4 algorithm, as presented in our previous work, is its encode complexity<sup>2</sup>. For example, compressing one rasterized, 15-layer layout of a 10 mm × 10 mm chip would take 2000 processor-months. This can be attributed to the exhaustive search nature of the segmentation portion of the C4 algorithm.

In this paper, we present two variations of the basic C4 algorithm. In Section 2, we present an overall structure of C4 algorithm. In Section 3, we introduce Block C4 to improve the encode complexity of C4 by few orders of magnitude. As it turns out, Block C4 also results in lower decoder complexity. In Section 4, we replace the Hierarchical Combinatorial Coding (HCC) part of C4 with Golomb run-length coding, to obtain a lower decode complexity algorithm called Block Golomb Context Copy Coding (Block GC3). In Section 5, we discuss hardware implementation aspects of the decoder for Block C4 and Block GC3. In Section 6, we discuss area, power, and speed estimates of Block C4 and Block GC3 decoders for direct-write maskless lithography systems.

## 2. OVERVIEW OF C4

The basic concept underlying C4 compression is to integrate the advantages of two disparate compression techniques: local context-based prediction<sup>10</sup>, and Lempel-Ziv (LZ) style copying<sup>11</sup>. The premise is simple: assuming pixels are transmitted in raster order, if a pixel value can be copied from a pixel preceding it, then it does not need to be transmitted again. The encoder simply needs to specify to the decoder how to perform the copy. Likewise, if a pixel value can be predicted from its neighbors, then it does not need to be transmitted. The decoder simply applies the same prediction mechanism to calculate the pixel value. By avoiding redundant transmission of copied or predicted pixels, C4 achieves compression. For this to work, however, the encoder needs to send additional information to the decoder, the segmentation map and the error location map.

First, the encoder needs to decide whether copying or prediction is more advantageous; if copying is used, some information needs to be provided as to where to copy from, e.g. from 5 pixels to the left or from the row above. This information is represented as a *segmentation map*, and represents *additional information* that must be transmitted from the encoder to the decoder. Clearly, generating segmentation on a per-pixel basis would increase the amount of information in the segmentation map to such an extent, that it may exceed the size of the uncompressed original image. To achieve a high compression rate, the C4 encoder must carefully group individual pixels into *copy regions* and *prediction regions*. In the case of C4, *copy regions* are defined as non-overlapping rectangles. Each copy region is represented as 4 coordinates  $(x, y, w, h)$ , where  $x$  and  $y$  represent the position of the rectangle, and  $w$  and  $h$  represent the width and height, respectively. In addition, 2 parameters are used to specify how to perform the copy  $(dir, d)$ , where  $dir$  represents the direction to copy from, left or above, and  $d$  represents the distance in pixels. Thus, in total, 6 parameters are associated with each copy region. The prediction region is, by definition, any pixel not included in a copy region.

The automatic segmentation of a layout into copy and prediction regions by the encoder is an extremely compute intensive task, and is vital to the compression efficiency of C4. Later, in Section 3, we examine in detail how and why this is the case, and present a new method called Block C4, which applies a lower complexity segmentation algorithm. Fortunately, for application to the maskless lithography datapath in Figure 1, the segmentation complexity does not affect the decoder, as it simply receives the segmentation map from the encoder.

In addition to segmentation, the encoder needs to specify to the decoder the location and value of *error pixels*. To increase the compression efficiency of C4, we deliberately allow some pixels in the copy or prediction regions to be erroneous, with the intention of correcting them at a later stage. For example, if a large region is nearly an identical copy of a previously encoded region with the exception of few pixels, it is still advantageous to classify it as a copy region provided the pixels in error are taken care of. These incorrectly copied or predicted pixels are called *error pixels*, and their location and values must also be transmitted from encoder to decoder. The locations of these error pixels are represented by a binary *error location map*, where a “0” indicates a correctly predicted/copied pixel, and a “1” indicates an error pixel. This error location map can be compressed with any standard binary compression technique, such as arithmetic coding. In C4, we use Hierarchical Combinatorial Coding (HCC), a low-complexity alternative to arithmetic coding proposed in our previous work<sup>3</sup>. Later in Section 4, we examine an alternative to HCC for compressing the error

location map, Golomb coding, and evaluate its effect on decoder complexity and compression efficiency. In addition, the value of error pixels, i.e. “error values” must also be transmitted from encoder to decoder. Error values are compressed using any entropy coding technique, such as Huffman coding.

The number of error pixels has a direct effect on the compression efficiency of C4. Fewer error pixels translate to fewer *error values* to be encoded. It also translates to fewer “1’s in the error location map, resulting in higher compression efficiency for HCC. Consequently, the goal of the C4 encoder is to minimize the frequency of error pixels, which is determined entirely by two factors: the properties of the layout itself, and the efficacy of the segmentation algorithm in taking advantage of these properties.

## 2.1. Factors affecting the compression efficiency of C4

At the beginning of this section we stated that “the basic concept underlying C4 compression is to integrate the advantages of two disparate compression techniques: local context-based prediction, and LZ-style copying.” Why should this strategy be advantageous for compressing layout? First, layout generated by layout designers are mostly Manhattan structured. This means that the majority of pixels may be classified as part of a vertical edge, horizontal edge, or a region of constant intensity. In context-based prediction, C4 examines neighboring pixels of a given pixel in order to determine whether it is part of an edge, or a region of constant intensity, and makes a prediction accordingly. Given the raster scan ordering, horizontal edges continue right, vertical edges continue down, and constant intensity regions remain the same color. This prediction mechanism typically fails only at corners of polygons, so the number of prediction error pixels is proportional to the number of polygon vertices. Therefore, for sparse features, it is advantageous to apply predictions, as empirically verified<sup>5</sup>.

For non-sparse layouts, such as dense memory layouts, C4 takes advantage of the fact that a single cell is replicated many times in the layout. After one cell pattern is encoded with prediction, the remainder can be generated with copying. Consequently, for dense repetitive features, it is advantageous to apply copy regions, also verified empirically<sup>5</sup>.

In general, a layout contains a heterogeneous mix of sparse irregular features, and dense repetitive features. It is the task of the C4 encoder to appropriately place as few copy regions as possible, in order to capture the repetitive features, so as

to minimize the total number error pixels. This is done with a greedy heuristic search algorithm that attempts to find few copy regions with maximal coverage of the layout, resulting in a minimum number of error pixels<sup>2</sup>. A high level overview of the algorithm is presented in Section 3.

## 2.2 Block diagram of the C4 encoder and decoder

Figure 2 shows a high-level block diagram of the C4 encoder and decoder for flattened, rasterized gray-level layout images. First, a prediction error image is generated from the layout, using a simple three-pixel prediction model to be described shortly. Next, the “Find copy regions” block uses the error image to do automatic segmentation as described above, generating a segmentation map between copy regions and the prediction regions. As specified by the segmentation, the predict/copy block estimates each pixel value, either by copying or by prediction. The result is compared to the actual value in the layout image. Correct pixel values are indicated with a “0” and incorrect values are indicated with a “1. The pixel error location is compressed without loss by the HCC encoder, and the corresponding pixel error value is compressed by the Huffman encoder. These compressed bit streams are transmitted to the decoder, along with the segmentation map.

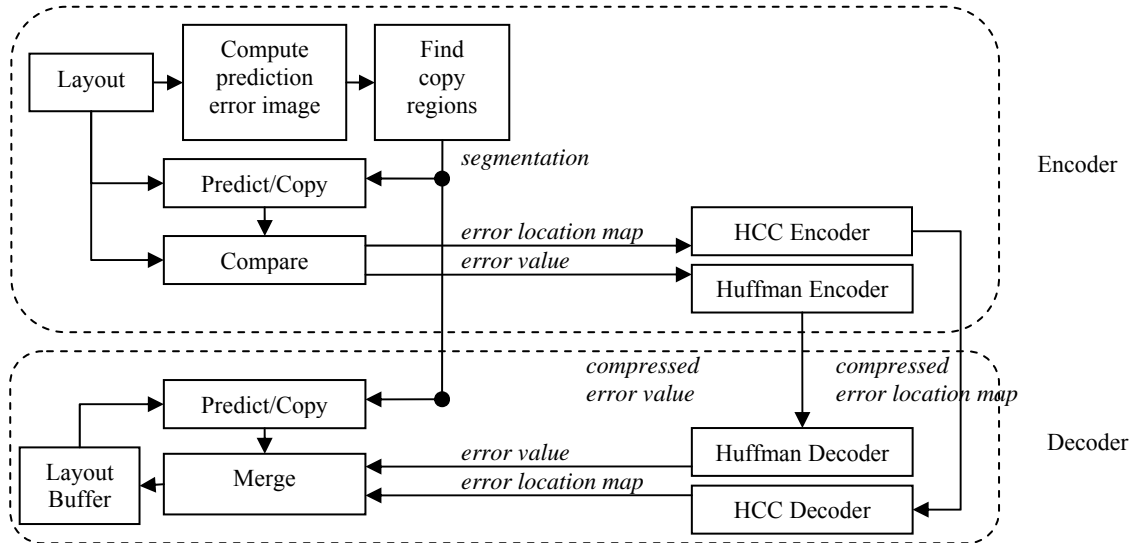


Figure 2. Block diagram of C4+LP encoder and decoder for grey-pixel images.

The decoder mirrors the encoder, but skips the complex process necessary to find the segmentation map, which is received from the encoder. The HCC decoder decompresses the error location bits from the encoder. As specified by the segmentation, the Predict/Copy block estimates each pixel value, either by copying or by prediction. If the error location bit is “0”, the pixel value is correct, and if the error location bit is “1”, the pixel value is incorrect, and must be replaced by the actual pixel value decoded from Huffman decoder. There is no segmentation performed in the C4 decoder, so it is considerably simpler to implement than the encoder, satisfying one of the requirements of the data path architecture in Figure 1.

The prediction algorithm used is linear prediction, where each pixel is predicted from its three-pixel neighborhood as shown in Figure 3. Pixel  $z$  is predicted as a linear combination of its local 3-pixel neighborhood  $a$ ,  $b$ , and  $c$ . If the prediction value is negative or exceeds the maximum allowed pixel value  $\max$ , the result is clipped to 0 or  $\max$  respectively. The intuition behind this predictor is simple: pixel  $b$  is related to pixel  $a$ , the same way pixel  $z$  relates to pixel  $c$ . For example, if  $b = a$ , as in a region of constant intensity, then predicting  $z = c$  continues that region of constant intensity. Also, if there is a step up from  $a$  to  $b$ , such that  $a + d = b$ , as in a vertical edge, then predicting an equivalent step up from  $c$  to  $z$ , such that  $c + d = z$ , continues that vertical edge. Likewise, if there is a step up from  $a$  to  $c$ , such that  $a + d = c$ , as in a horizontal edge, then predicting an equivalent step up from  $b$  to  $z$ , such that  $b + d = z$ , continues that horizontal edge. Thus, these equations predict a continuation of horizontal edges, vertical edges, and regions of constant intensity. Interestingly, this linear predictor can also be applied to a binary image by setting  $\max = 1$ , resulting in the same predicted values as binary context-based prediction proposed in our previous work<sup>2</sup>. It is also similar to the median predictor used in JPEG-LS<sup>10</sup>. The linear prediction is used in both encoder and decoder, as shown in Figure 2.

$a$	$b$
$c$	$z$

$$x = b - a + c$$

$$\text{if}(x < 0) \text{ then } z = 0$$

$$\text{if}(x > \max) \text{ then } z = \max$$

$$\text{otherwise } z = x$$

Figure 3. Three-pixel linear prediction with saturation used in grey-pixel C4.

### 3. BLOCK C4

Block C4 is an improvement over the C4 compression algorithm<sup>2</sup>. Similar to C4, it is designed to compress flattened, rasterized layout data, and provides similar compression efficiency but at a tiny fraction of the encoding time. In Table 1, we compare the compression efficiency and encoding time for two  $1024 \times 1024$  5-bit grayscale layout images, generated from two different sections of the poly layer of a layout. The flavor of C4 used here and throughout this paper is C4+LP, the variant of C4 with the lowest decoder implementation complexity. LP stands for linear prediction of a pixel based on its surrounding pixels as described in Section 2. Encoding times are generated on an AMD Athlon64™ 3200+ Windows XP desktop with 1 GB of memory. As seen, Block C4 is 115 times faster for the Poly-memory layout, and 865 times faster on the Poly-control layout with no noticeable loss in compression efficiency. There are some layouts for which Block C4 has significantly less compression efficiency, but the speed advantage is universal. A more complete table of results appears in Table 2 of subsection 3.4.

Table 1. Comparison of compression ratio and encode times of C4 vs. Block C4.

Layout	C4 Compression Ratio	C4 Encode Time	Block C4 Compression Ratio	Block C4 Encode Time
Poly-memory	7.60	1608 s (26.8 min)	7.63	14.0 s (115x speedup)
Poly-control	9.18	12113 s (3.4 hrs)	9.18	13.9 s (865x speedup)

The significance of a speedup of this magnitude in encoding time cannot be understated. Indeed, if we extrapolate from an average encoding time of 30 minutes per  $1024 \times 1024$  layout image, a 20mm  $\times$  10mm chip die drawn on a 22 nm 5-bit grayscale grid would take over 22 CPU years to encode. Block C4 reduces this to number to 60 CPU days, still a large number, but manageable by today's multi-core, multi-CPU compute systems.

Another benefit of Block C4, apparent in Table 1, is an approximately constant computation time of about 14 seconds per  $1024 \times 1024$  layout image, independent of the layout data, as compared to widely varying computation times of C4, from 27 minutes to 3.4 hours. A predictable and consistent computation time is important to project planning, for example, to maximize tool usage.

The remainder of this section describes how Block C4 achieves this encoding speedup with no loss in compression efficiency. In Section 3.1, we introduce the segmentation algorithm of C4 and contrast it with Block C4. In Section 3.2,

we examine the problem of choosing a block size for Block C4. In Section 3.3, we describe how the Block C4 segmentation is encoded for compression efficiency.

### 3.1. Segmentation in C4 vs. Block C4

The basic concept underlying both C4 and Block C4 compression is exactly the same. Layout data is characterized by a heterogeneous mix of repetitive and non-repetitive structures, examples of which are shown in Figures 4(a) and 4(b) respectively. Repetitive structures are compressed efficiently using LZ-style copying, whereas non-repetitive structures are better compressed using localized context-prediction techniques<sup>5</sup>. The task of both the C4 and Block C4 encoder is to automatically partition the image into repetitive copy regions, and non-repetitive prediction regions, in a process called *segmentation*. The result is a *segmentation map*, which indicates whether copy or prediction should be used to compress each pixel of the image. Once the segmentation into prediction versus copy is complete, it is straightforward to encode each pixel according to this segmentation map. The segmentation map must also be encoded and included as part of the compressed data, so that the decoder knows which algorithm to apply to each pixel for decoding.

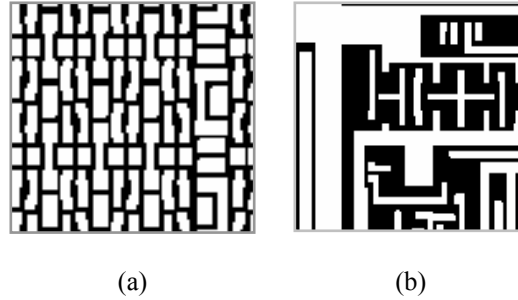


Figure 4. (a) Repetitive and (b) non-repetitive layouts.

The task of computing the segmentation map accounts for nearly all the computation time of the C4 encoder. Of the encode times reported in Table 1, the encode time excluding segmentation, is a constant 1.2 seconds, for both C4 and Block C4. In other words, over 99.9% of the encode time of C4 and 91% of the encode complexity of Block C4 is attributable to segmentation.

In C4, the segmentation is described as a list of rectangular copy regions. An example of a copy region is shown in Figure 5. Each copy region is a rectangle, enclosing a repetitive section of a layout, described by 6 attributes: the

rectangle position  $(x, y)$ , its width and height  $(w, h)$ , the orthogonal direction of the copy ( $dir = left$  or  $above$ ), and the distance to copy from  $(d)$  i.e. the period of the repetition.

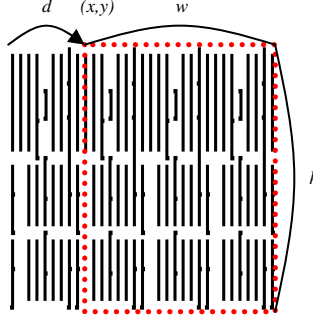


Figure 5. Illustration of a copy region.

What makes automated C4 segmentation such a complex task is that the “best” segmentation, or even a “good” segmentation is hardly obvious. Even in such a simple example shown in Figure 5, there are many potential copy regions, a few of which are illustrated in Figure 6 as dotted and dashed rectangles. The number of all possible copy regions is of the order of  $O(N^5)$  for  $N \times N$  pixel layout, and choosing the best set of copy regions for a given layout is a combinatorial problem. Exhaustive search in this space is prohibitively complex, and C4 already adopts a number of greedy heuristics to make the problem tractable<sup>2</sup>. Clearly further complexity reduction of the segmentation algorithm is desirable.

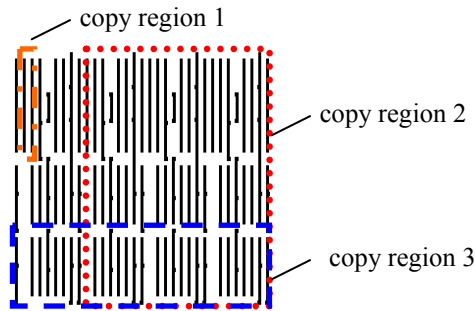


Figure 6. Illustration of a few potential copy regions that may be defined on the same layout.

Block C4 adopts a far more restrictive segmentation algorithm than C4, and as such, is much faster to compute. Specifically, Block C4 restricts both the position and sizes to fixed  $M \times M$  blocks on a grid whereas C4 allows for copy regions to be placed in arbitrary  $(x,y)$  positions with arbitrary  $(w,h)$  sizes. Figure 7 illustrates the difference between Block C4 and C4 segmentation. In Figure 7(a), the segmentation for C4 is composed of 3 rectangular copy regions, with 6 attributes  $(x,y,w,h,dir,d)$  describing each copy region. In Figure 7(b), the segmentation for Block C4 is composed of 20  $M \times M$  tiles, with each tile marked as either prediction ( $P$ ), or the copy with direction and distance ( $dir, d$ ). This simple change reduces the number of possible copy regions to

$$O\left(\frac{N^3}{M^2}\right) \sim \frac{N^2}{M^2} \times O(N),$$

a substantial  $N^2M^2$  reduction in search space compared to C4. For the experiment in Table 1, we have  $N = 1024$  and  $M = 8$ , so the copy region search space has been reduced by a factor of 64 million. However, this complexity reduction could potentially come at the expense of compression efficiency.

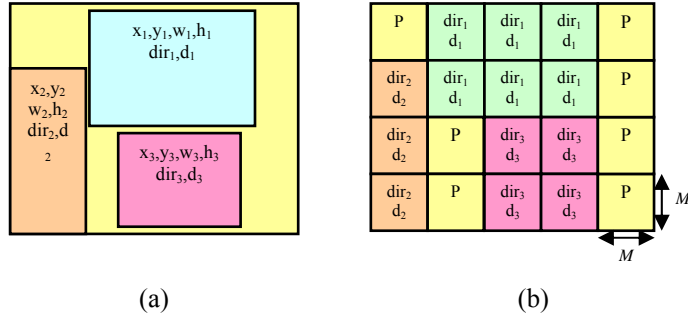


Figure 7. Segmentation map of (a) C4 vs. (b) Block C4.

### 3.2. Choosing a block size for Block C4

The three large copy regions in C4 segmentation map in Figure 7(a) have been divided into 13 small square blocks in Block C4 in Figure 7(b) in this example. In general, a large repetitive  $w \times h$  region is broken up into  $wh/M^2$  tiles in Block C4. Each copy region tile in Block C4 is represented with only 2 attributes ( $dir, d$ ) rather than the 6 per copy region  $(x,y,w,h,dir,d)$  in C4. If a sufficiently large tile is broken up, there may be a net increase in the amount of data needed to

represent the segmentation information, which adversely affects the compression ratio of Block C4. Smaller values of  $M$  accentuate this effect, motivating the use of larger  $M$ .

However, large values of  $M$  could also be disadvantageous. Comparing the segmentation map of C4 in Figure 7(a) to that of Block C4 in Figure 7(b), the rectangles are forced to snap to the coarse grid in Block C4. In C4, the rectangle boundaries are optimized to delineate repetitive regions from non-repetitive regions. In Block C4, the coarse grid causes this delineation to be sub-optimal. Consequently, at the boundary of the copy regions, repetitive regions are predicted, and non-repetitive regions are copied. This sub-optimal segmentation could potentially lower the compression efficiency. Of course, the smaller and finer the grid, the lower the occurrence of grid snapping, hence motivating the use of a smaller  $M$ .

These arguments suggest that there is an optimal  $M$  value that trades off between grid snapping and the breakup of large copy regions. We have empirically found  $M = 8$  to exhibit the best compression efficiency for nearly all test cases as compared to  $M = 4$  or  $M = 16$ . In the remainder of this paper, we use  $M = 8$  in all of our Block C4 experimental results, unless otherwise stated.

### 3.3. Context-based block prediction for encoding Block C4 segmentation

To further improve the compression efficiency of Block C4, we note that the segmentation shown in Figure 7(b) is highly structured. Indeed, the segmentation can be used to represent boundaries in a layout separating repetitive regions from non-repetitive regions, and that these repetitions are caused by design cell hierarchies, which are placed on an orthogonal grid. Consequently, Block C4 segmentation has an orthogonal structure, and C4 already employs a reasonably efficient method for compressing orthogonal structures placed on a grid, namely context-based prediction<sup>2</sup>.

To encode the segmentation, blocks are treated as pixels, and the attributes  $(P, dir, d)$  as colors of each block. Each block is predicted from its three-block neighborhood, as shown in Figure 8. For vertical edges corresponding to  $c = a$ , it is likely for  $z$  to be equal to  $b$ . Similarly for horizontal edges corresponding to  $a = b$ , it is likely for  $z$  to be equal to  $c$ . Consequently, the prediction shown in Figure 8 only fails around corner blocks, which are assumed to occur less frequently than horizontal or vertical edges. Applying context-based block prediction to the segmentation in Figure 9(a),

we obtain Figure 9(b) where  $\checkmark$  marks indicate correct predictions. The pattern of  $\checkmark$  marks could be compressed using HCC<sup>3</sup> or any other binary coding techniques, and the remaining values of  $(P, dir, d)$  could be Huffman coded, exactly analogous to the method of coding copy/prediction error bits and values used in C4<sup>2</sup>. For Block C4, we choose to use Golomb run-length coder to compress segmentation error locations. This is because the segmentation error location amounts to a very small percentage of the output bit stream, and as such, applying a complex scheme such as HCC is hard to justify.

$a$	$b$
$c$	$z$

*If*( $c = a$ ) *then*  $z = b$   
*else*  $z = c$

Figure 8. Three-block prediction for encoding segmentation in Block C4.

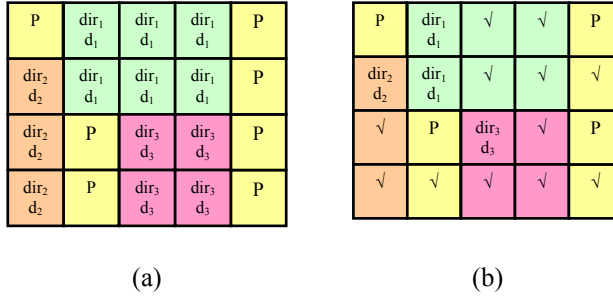


Figure 9 consists of two tables, (a) and (b), showing segmentation maps for Block C4. Both tables have five columns: P, dir<sub>1</sub> d<sub>1</sub>, dir<sub>1</sub> d<sub>1</sub>, dir<sub>1</sub> d<sub>1</sub>, and P.

P	dir <sub>1</sub> d <sub>1</sub>	dir <sub>1</sub> d <sub>1</sub>	dir <sub>1</sub> d <sub>1</sub>	P
dir <sub>2</sub> d <sub>2</sub>	dir <sub>1</sub> d <sub>1</sub>	dir <sub>1</sub> d <sub>1</sub>	dir <sub>1</sub> d <sub>1</sub>	P
dir <sub>2</sub> d <sub>2</sub>	P	dir <sub>3</sub> d <sub>3</sub>	dir <sub>3</sub> d <sub>3</sub>	P
dir <sub>2</sub> d <sub>2</sub>	P	dir <sub>3</sub> d <sub>3</sub>	dir <sub>3</sub> d <sub>3</sub>	P

P	dir <sub>1</sub> d <sub>1</sub>	$\checkmark$	$\checkmark$	P
dir <sub>2</sub> d <sub>2</sub>	dir <sub>1</sub> d <sub>1</sub>	$\checkmark$	$\checkmark$	$\checkmark$
$\checkmark$	P	dir <sub>3</sub> d <sub>3</sub>	$\checkmark$	P
$\checkmark$	$\checkmark$	$\checkmark$	$\checkmark$	$\checkmark$

(a)

(b)

Figure 9. (a) Block C4 segmentation map (b) with context-based prediction.

### 3.4. Compression results for Block C4

As we have seen in the previous sub-sections, Block C4 speeds up C4 by introducing a coarse fixed grid of  $8 \times 8$  pixel blocks for the segmentation. This change dramatically reduces the size of the search space for copy regions, resulting in a large speedup of the encoding time. Even though the coarse grid results in lowered compression efficiency, we have mitigated this by an appropriate choice of the block size, and the application of the context-based block prediction. The full table of results, comparing Block C4 to C4 is shown in Table 2. In it, we compare the compression efficiency and encoding time of various  $1024 \times 1024$  5-bit grayscale images, generated from different sections and layers of an industry microchip. In columns, from left to right, are the layer image name, C4 compression ratio, C4 encode time, Block C4

compression ratio, and Block C4 encode time. Both C4 and Block C4 use the smallest 1.7 kB buffer, corresponding to only 2 stored rows of data. Encoding times are generated on an AMD Athlon64<sup>TM</sup> 3200+ Windows XP desktop with 1 GB of memory.

Table 2. Comparison of compression ratio and encode times of C4 vs. Block C4.

Layout	C4 Compression Ratio	C4 Encode Time	Block C4 Compression Ratio	Block C4 Encode Time
Poly-memory	7.60	1608 s (26.8 min)	7.63	14.0 s (115x speedup)
Poly-control	9.18	12113 s (3.4 hrs)	9.18	13.9 s (865x speedup)
Poly-mixed	10.6	1523 s (25.4 min)	11.35	13.9 s (110x speedup)
M1-memory	13.1	3841 s (1.1 hrs)	9.50	13.9 s (276x speedup)
M1-control	18.7	13045 s (3.6 hrs)	17.3	13.9 s (938x speedup)
M1-mixed	15.5	13902 s (3.9 hrs)	14.7	13.9 s (1000x speedup)
Via-dense	10.2	3350 s (55.8 min)	15.5	14.1 s (237x speedup)
Via-sparse	16.0	7478 s (2.1 hrs)	21.6	13.7 s (546x speedup)

A quick glance at this table makes clear the speed advantage of Block C4 over C4 is universal, i.e. over 100 times faster than C4, and consistent, i.e. 13.7 to 14.1 seconds, for all layers and layout types tested. In general, the compression

efficiency of Block C4 matches that of C4. One exception is row 5 of Table 2, where C4 exceeds the compression efficiency of Block C4, on the highly regular M1-memory layout.

For this layout, C4's compression ratio is 13.1, while Block C4's compression ratio is 9.5. In this particular case, the layout is extremely repetitive, and C4 covers 99% of the entire  $1024 \times 1024$  image with only 132 copy regions. Moreover, many of these copy regions are long narrow strips, less than 8-pixels wide, which Block C4 cannot possibly duplicate. Consequently, Block C4 exhibits a loss of compression efficiency as compared to C4, in this particular case.

On the other hand, in the last two rows of Table 2, the compression ratio of Block C4 exceeds the compression ratio of C4 for the dense and sparse “Via” layout. The Via layer consists of a large number of small squares scattered like flakes across the image. It is best compressed with a large number of small copy regions, each covering a few squares. Block C4 has two advantages in this case: it uses fewer bits to represent each copy region than C4, and it takes advantage of correlations between copy regions, using context-based block prediction. For example, in the Via-sparse layer image, C4 applies 945 copy regions to cover ~50% of the layout. In contrast, Block C4 covers ~96% of the same image with copy regions, thereby achieving significantly higher compression ratio.

#### 4. BLOCK GC3—ALTERNATE WAY TO COMPRESS THE ERROR LOCATION

In both C4 and Block C4, the error location bits are compressed using HCC. While HCC is useful for encoding the highly-skewed binary data in a lossless fashion<sup>3</sup>, when it comes down to hardware implementation, the hierarchical structure of HCC implies repetitive hardware blocks and inevitable decoding latency from the top level to the final output. Moreover, as we show in Section 6, the HCC block becomes the bottleneck of the entire system due to its long delay. To overcome this problem, we propose to replace HCC in Block C4 by a Golomb run-length coder<sup>8</sup>, resulting in a new compression algorithm called Block GC3. As such, Golomb run-length coder in Block GC3 is now used to encode error locations of both the pixels in the layout and the segmentation blocks in the segmentation map. Figure 10 shows the block diagram for Block GC3, which is more or less identical to that of C4 shown in Figure 2 with the exception of the pixel error location encoding scheme and segmentation map compression as discussed in the previous section.

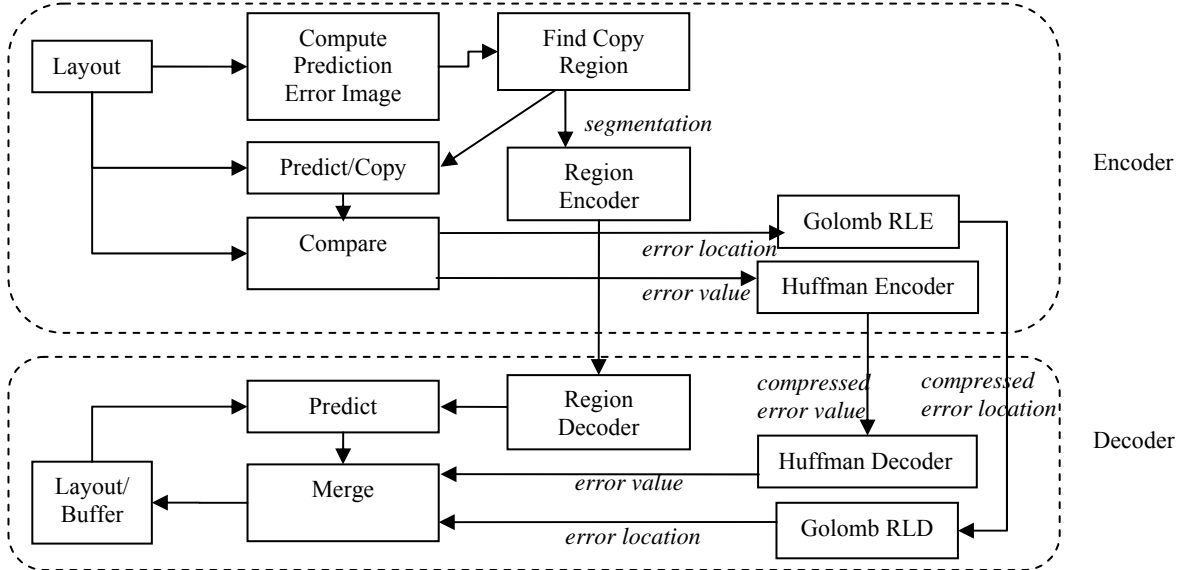


Figure 10. The encoding/decoding architecture of Block GC3.

Coding the pixel error location of layouts with Golomb run-length code could potentially lower the compression efficiency. Figure 11 shows a binary stream coded with both HCC and Golomb run-length coder. In the upper path, the stream is coded with Golomb run-length coder. In this case, the input stream is either coded as (0), denoting a stream of  $B$  zeroes ,where  $B$  denotes a predefined bucket size, or coded as (1,  $n$ ), indicating a “1” occurs after  $n$  zeroes. In general, the algorithm of Golomb code requires integer multiplication and division. To simplify it to bit-shifting operation, we restrict  $B$  to be power of 2. These parameters are further converted into a bit stream, where parameter (0) is translated into a 1-bit codeword and (1,  $n$ ) takes  $1 + \log_2 B$  bits to encode. Therefore, a stream with successive ones can potentially be encoded into a longer code than a stream with ones which are far apart from each other. On the other hand, in the lower path of Figure 11, HCC counts the number of ones within a fixed block size and codes it using enumerative code<sup>2</sup>. In Fig. 11, the block size is 8 and attributes (2, 11) denote the 11<sup>th</sup> greatest 8-bit sequence with two “1”s, i.e. “01000010.” The attributes (2, 11) are further translated to codewords “010” and “01011,” which are the binary representations of 2 and 11 respectively. As long as the number of ones inside the block is fixed, HCC results in a fixed length bit stream regardless of the input distribution.

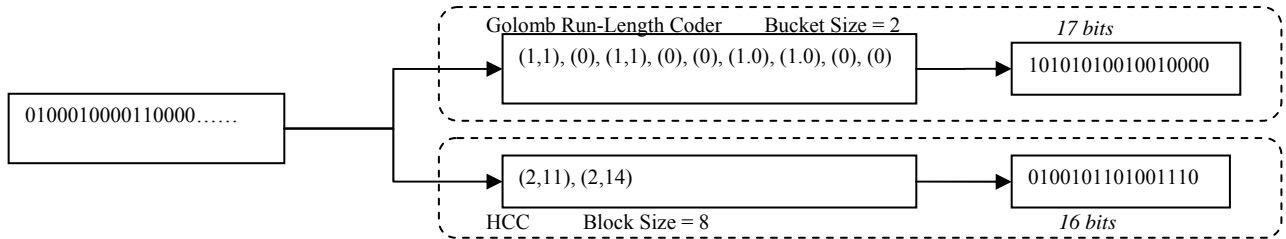


Figure 11. Golomb run-length encoding process.

Based on the above, Block GC3 can result in potential compression efficiency loss for certain class of images. Specifically, Figure 12 shows a typical layout with successive prediction errors occurring at the corner of Manhattan shapes due to the linear prediction property. Since error locations are not distributed in an independent-identically distributed (i.i.d.) fashion, there is potential compression efficiency loss due to Golomb run-length coder as compared to HCC. To alleviate this problem, we adapt the bucket size for Golomb run-length coder from layer to layer.

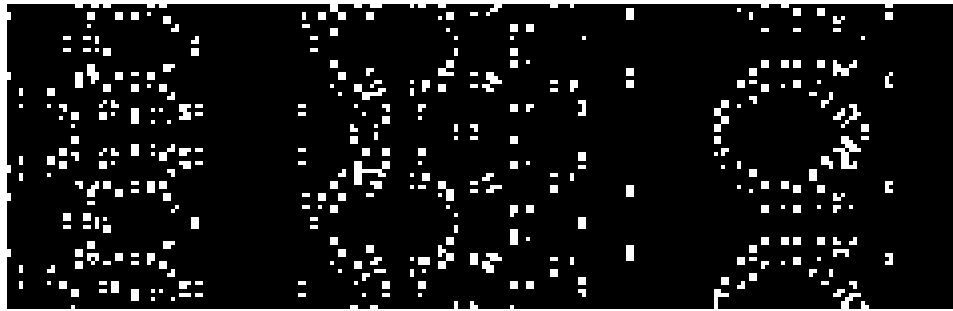


Figure 12. Visualization of pixel error location for a layout image.

As shown in Table 3, Block GC3 results in about 10 to 15 % lower compression efficiency than Block C4 over different process layers of layouts assuming decoder buffer size of 1.7 kB. The test images in Table 3 are  $1024 \times 1024$  5-bit grayscale rasterized, flattened layouts, examples of which are shown in Figures 4(a) and 4(b). Similarly, Figure 13 compares the minimum compression efficiency of Block C4, Block GC3, and few other existing lossless compression schemes as a function of decoder buffer size<sup>1</sup>. The minimum is computed over ten  $1024 \times 1024$  images manually selected among five layers of two IC layouts. In practice, we focus on 1.7 kB buffer size for hardware implementation purposes.

While Block GC3 results in slightly lower compression efficiency than Block C4 for nearly all decoder buffer sizes, it outperforms all other existing lossless compression schemes such as LZ77, ZIP, BZIP2, Huffman, and RLE.

Table 3. Compression ratio comparison between Block C4 and Block GC3 for different layers of layout.

Layers	Compression Ratio (Block C4)	Compression Ratio (Block GC3)	Bucket size for Block GC3
Metal 1 mixed	14.21	12.67	16
Metal 2 mixed	33.81	28.83	64
N active mixed	43.10	36.51	64
P active mixed	66.17	59.24	128
Poly mixed	11.00	9.633	16

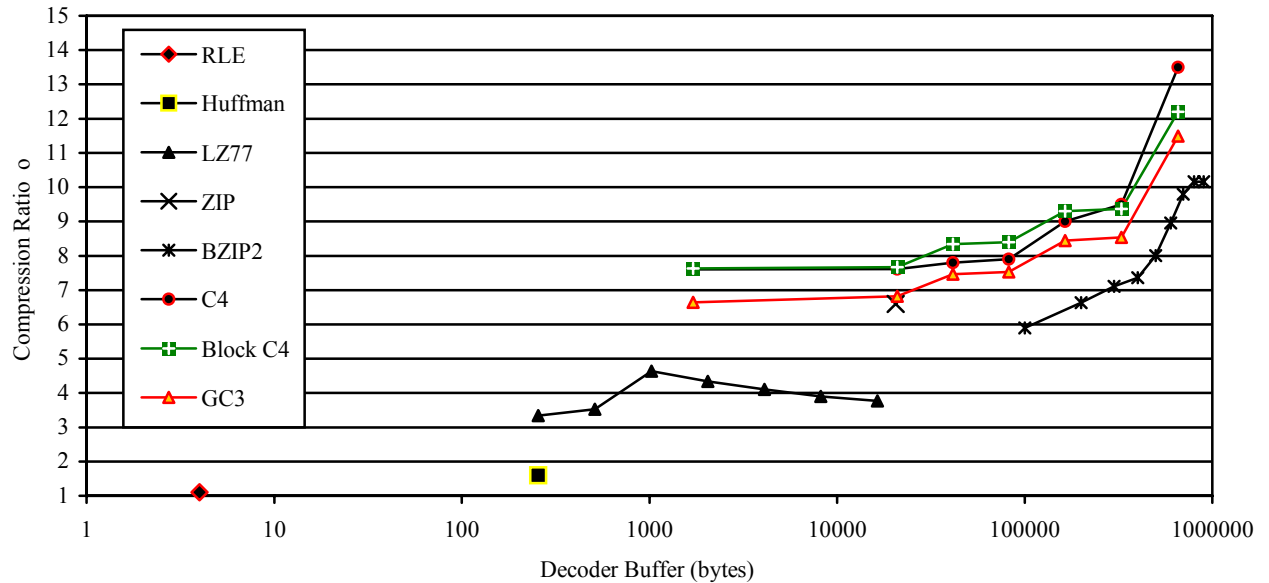


Figure 13. Compression efficiency and buffer size tradeoff for Block C4 and Block GC3.

## 5. DECODER ARCHITECTURE

For the decoder to be used in a maskless lithography data path, it must be implemented as a custom digital circuit and included on the same chip with the writer array. In addition, to achieve a system with high level of parallelism, the

decoder must have the data-flow architecture and high throughput. By analyzing the functional blocks of the Block C4 and Block GC3 algorithms, we devise the data-flow architecture for the decoder<sup>1</sup>.

The block diagram of Block C4 decoder is shown in Figure 14. There are three main inputs: the segmentation, the compressed error location, and the compressed error value. The segmentation is fed into the Region Decoder, generating a segmentation map as needed by the decoding process. Using this map, the decoded predict/copy property of each pixel can be used to select between the predicted value from Linear Prediction and the copied value from History Buffer in the Control/Merge stage by a multiplexer (MUX), as shown in Figure 15. The compressed pixel error location is decoded by HCC, resulting in an error location map, which indicates the locations of invalid predict/copy pixels. In the decoder, this map contributes to another control signal in the Control/Merge stage to select the final output pixel value from either predict/copy value or the decompressed error value generated by Huffman decoder. The output data is written back to History Buffer for future usage, either for linear prediction or for copying, where the appropriate access position in the buffer is generated by the Address Generator. All the decoding operations are combinations of basic logic and arithmetic operations, such as selection, addition, and subtraction. By applying the tradeoffs described in Section 4, the total amount of needed memory inside a single Block C4 decoder is about 2 KB, which can be implemented using on-chip SRAM.

The block diagram of Block GC3 is almost identical to that of Block C4 shown in Figure 14, since it only replaces the HCC block of Block C4 by a Golomb run-length decoder.

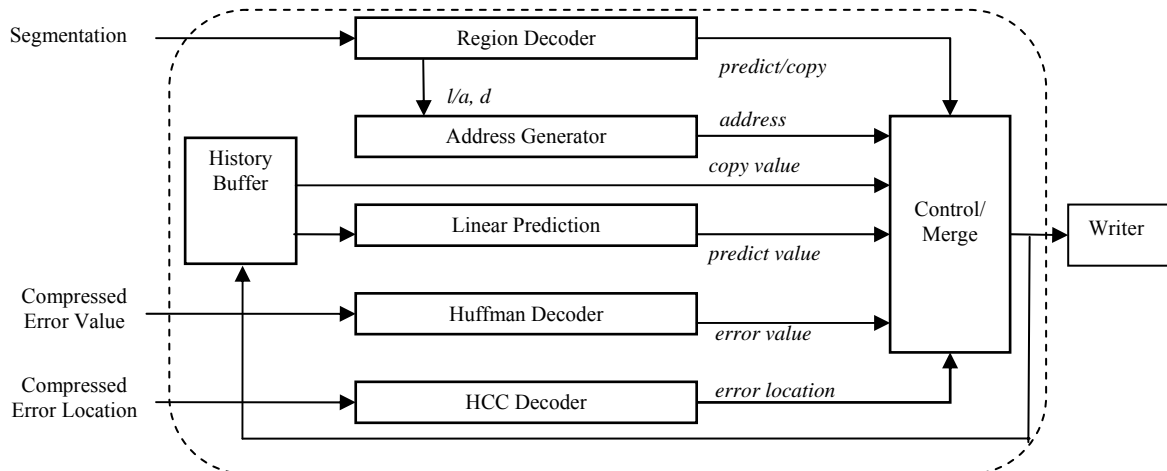


Figure 14. Functional block diagram of Block C4 decoder.

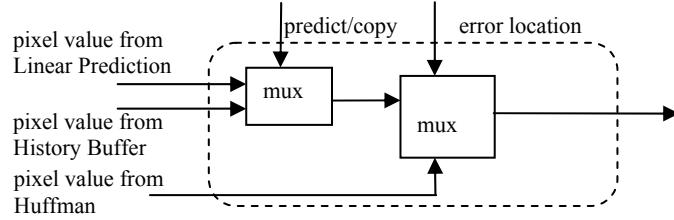


Figure 15. Block diagram of Merge/Control block.

In the remainder of this section, we discuss the architecture for the Block C4 and Block GC3 decoders. Even though there are seven major blocks shown in Figure 14, we focus on the two most challenging blocks of the design, namely the Region Decoder and HCC. For Block GC3, we only discuss the design of Golomb run-length decoder, as its main distinctive feature.

### 5.1. Region decoder

In the description of the Block C4 algorithm in Section 3, a segmentation map is introduced to represent the predict/copy segmentation of the layout. Similar to an actual IC layout, the segmentation map is also Manhattan shaped, and can be compressed by prediction algorithms. However, since the segmentation map is an artificially generated image, there is no correlation between the values of adjacent segments. As a result, the segmentation predictor shown in Figure 8 is used in the Region Decoder rather than the linear predictor used for pixel predictions in a layout.

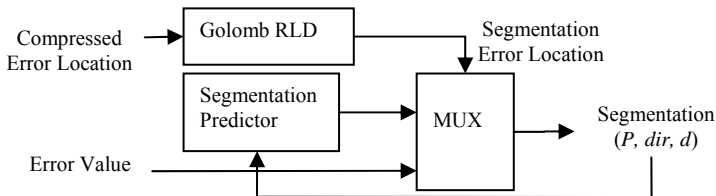


Figure 16. Block diagram of Block C4 Region Decoder.

Figure 16 shows the block diagram of the Region Decoder for Block C4. The segmentation input has been separated into two streams, the compressed error location and the error value. The core of the Region Decoder is the segmentation

predictor. As shown in Figure 16, the output of the Region Decoder is selected to be either the error value or the output of the segmentation predictor, depending upon the segmentation error location provided by the Golomb run-length decoder. Similar to the linear predictor for the layout image, the segmentation predictor of Block C4 applies the three-block-based prediction: the segmentation of the current micro-block is determined by the three adjacent blocks from upper, left, and upper left micro-blocks under the conditions shown in Figure 8.

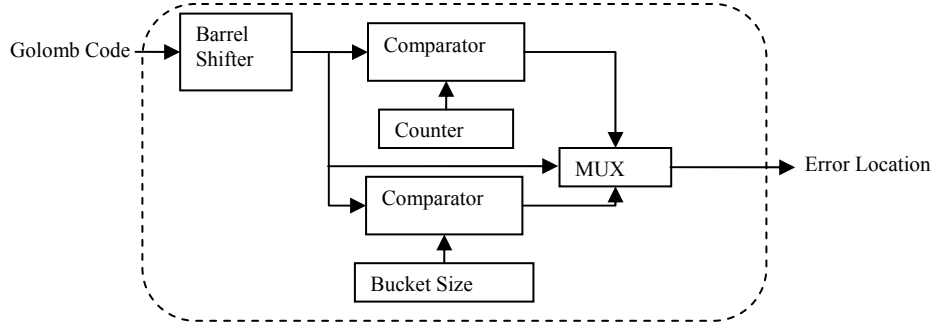


Figure 17. Block diagram of Golomb run-length decoder.

The design of Golomb run-length decoder is adapted from techniques in the existing literature<sup>9</sup>, as shown in Figure 17. It is the combination of a barrel shifter and a conventional run-length decoder. The barrel shifter is used as a data buffer to compact the coded error location into an 8-bit data stream, and the decoded result is used as the input to a run-length decoder, resulting in a binary output stream. In contrast to the approach in the literature, we only use one barrel shifter in our design in order to reduce the hardware overhead.

The proposed Region Decoder has several architectural advantages over the original C4 Region Decoder<sup>1</sup>. First, it is implemented as a regular data path, in contrast to a linked-list structure, thus eliminating feedback and latency issues. Second, the output of Block C4 Region Decoder is the control signal over an 8x8 micro-block, which lowers the output rate of Region Decoder by 64, and reduces the power consumption. Finally, the length of the segmentation parameter is reduced from 51 bits ( $[x, y, w, h, dir, dist]$ ) to 19 bits, i.e. 8-bit error location and 11-bit error value, resulting in fewer I/O pins in the decoder.

## 5.2. HCC block design

Combinatorial coding (CC) is an algorithm for compressing a binary sequence of 0's and 1's. For Block C4, it represents a binary pixel error location map. A “0” represents a correctly predicted or copied pixel, and a “1” represents a prediction/copy error. CC encodes this data by dividing the bit sequence into blocks of fixed size  $H$ , e.g.  $H = 4$ , and computing  $k_{\text{block}}$  the number of “1”s in each block. If  $k_i = 0$ , this means block  $i$  has no ones, so it is encoded as 0000, with a single value  $k_i$ . If  $k_i > 0$ , e.g.  $k_i = 1$ , then it needs to be disambiguated between the list of possible 4-bit sequences with one “1”: {1000, 0100, 0010, 0001}. This can be done with an integer representing an index into that list denoted  $\text{rank}_{\text{block}}$ . In this manner, any block  $i$  of  $H$  bits can be encoded as a pair of integers  $(k_i, \text{rank}_i)$ . For example, (2, 3) represents the third greatest 4-bit sequence with two “1”s among all possibilities: {1100, 1010, 1001, 0110, 0101, 0011}, i.e. “1001.” The theoretical details of how this achieves compression can be found in our previous work<sup>3</sup>, but, intuitively it can be expressed as follows: if the data contains contiguous sequences of “0”s, and if the length of these all “0” sequences matches the block size  $H$ , each block of  $H$  “0”s can be concisely encoded as  $(k_i = 0)$  with no rank value, effectively compressing the data.

Computational complexity of CC grows as the factorial of the block size  $H$ . Hierarchical combinatorial coding (HCC) avoids this issue by limiting  $H$  to a small value, and recursively applying CC to create a hierarchy, as shown in Figure 18.

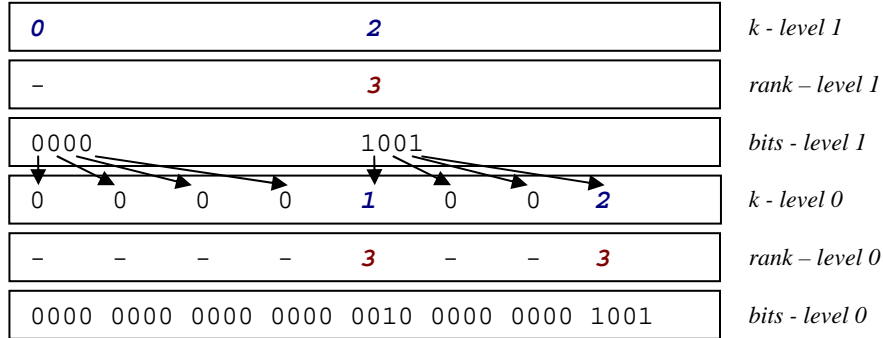


Figure 18. Two-level HCC with a block size  $H = 4$  for each level.

In Figure 18, the original binary sequence is the lowest row of the hierarchy “bits – level 0”. It has been encoded using CC as “k – level 0” and “rank – level 0” with a block size  $H = 4$ . We now recursively apply CC on top of CC by first

converting the integers in “k – level 0” to binary “bits – level 1” as follows: 0 is represented as 0, and non-zero integers are represented as 1. Applying CC to “bits – level 1” results in “k – level 1” and “rank – level 1”. The advantage of the hierarchical representation is that a single 0 in “k – level 1” now represents 16 zeros in “bits – level 0”. In general, a single 0 in “k - level  $L$ ” corresponds to  $H^{L+1}$  zeroes in “bits – level 0”, compressing large blocks of 0’s more efficiently. The disadvantage of decoding the HCC is that it requires multiple CC decoding steps, as we traverse the hierarchy from top to bottom.

The task of traversing the hierarchy of HCC decoding turns out to be the main throughput bottleneck of HCC decoder, which in turn is the throughput bottleneck of the entire Block C4 decoder. The block diagram of a sequential HCC decoder is shown in Figure 19(a). Block C4 uses a 3-level  $H = 8$  HCC decoder. The dashed lines separate the HCC levels from top to bottom, and the data that moves between levels are the “bits – level  $L$ .” Three CC blocks represent  $(k, rank)$  decoders for levels 2, 1, and 0, from top to bottom respectively. CC – level 2 decodes to bits – level 2. If bits – level 2 is a “0” bit, the MUX selects the run-length decoder (RLD) block which generates 8 zeros for “bits – level 1”. Otherwise, the MUX selects the CC – level 1 block to decode a  $(k, rank)$  pair. Likewise, “bits level – 1” controls the MUX in level 0. A “0” causes the RLD block to generate 8 zeros, and a “1” causes CC – level 0 to decode a  $(k, rank)$  pair. In this sequential design, the output of a lower level must wait for the output of a higher level to be available before it can continue. Consequently, the control signal corresponding to when the output of the lowest level “bits level – 0” is ready resembles Figure 19(c). While levels 2 and 1 are decoding as indicated by the shaded boxes, the output of layer 0 must stall, reducing the effective overall throughput of the HCC block.

To overcome the problem of HCC decoding, we can parallelize the operation by introducing a FIFO buffer between HCC levels, as indicated by the additional squares in Figure 19(b), and by dividing the input  $(k, rank)$  values for each HCC level into multiple sub-streams. The idea is that after an initial delay to fill the buffers of levels 2 and 1, level 0 can decode continually as long as the buffers are not empty. This is guaranteed because one level 2 output bit corresponds to 8 level 1 output bits, and 64 level 0 output bits. Level 2 and level 1 can continue to decode into these buffers while level 0 is working. Consequently, the output control signal of the parallel design resembles Figure 19(d), where only the initial delay is noticeable. The control mechanism of the parallel design is also considerably simpler than the sequential design,

because each HCC level can now be controlled independently of the other HCC levels, halting only when its output buffer is full, or its input buffer is empty. Only a 2-byte FIFO is introduced between each level.

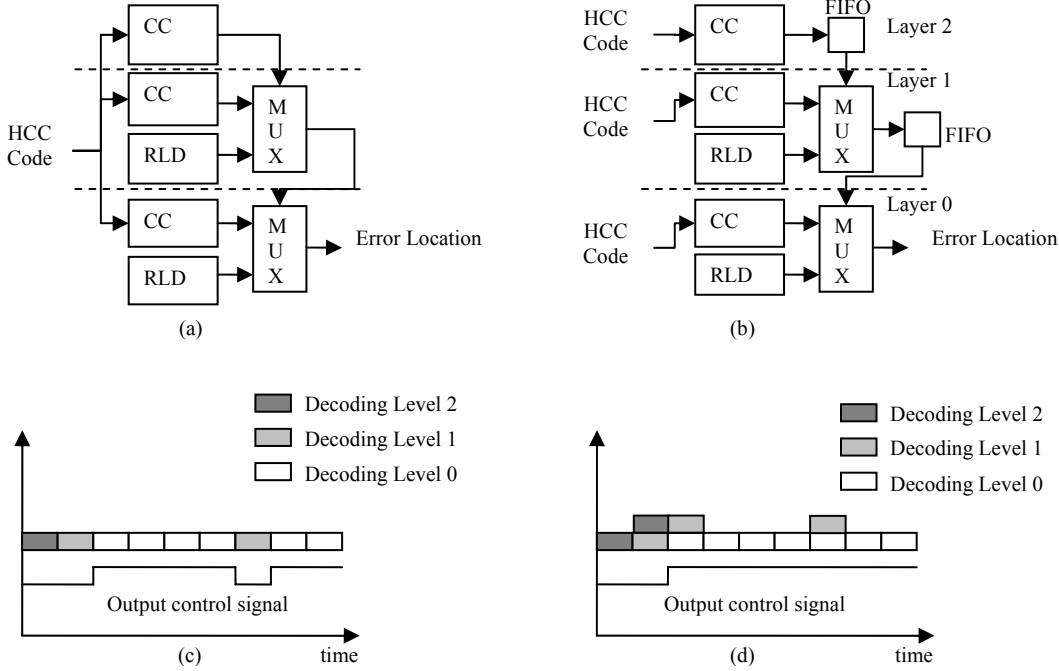


Figure 19. The decoding process of HCC in (a) top-to-bottom fashion and (b) parallel scheme. The timing analysis of (c) top-to-bottom fashion and (d) parallel scheme.

### 5.3. Golomb run-length decoder for Block GC3

Since the pixel error location in Block GC3 is encoded with Golomb run-length coder, the pixel error location decoder of Block GC3 resembles the Golomb run-length decoder for the segmentation map in the Region Decoder of Block C4. However, for pixel error locations, it is advantageous to use a variable bucket size in the Golomb run-length coder for different process layers in order to improve compression efficiency, as discussed in Section 3. The block diagram of Golomb run-length decoder for error location is shown in Figure 20. The only difference between Figures 17 and 20 is that the variable bucket size is introduced as an input signal to the decoder. The main advantage of this implementation over HCC is that it has zero latency, and does not require any stall cycles during the decoding process due to its regular data path structure.

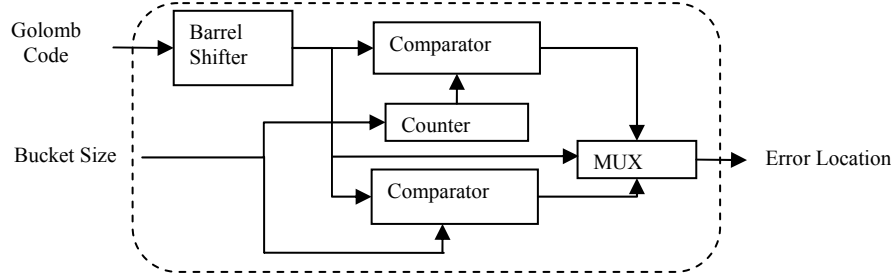


Figure 20. Block diagram of Golomb run-length pixel error location decoder in Block GC3.

## 6. DECODER PERFORMANCE

By applying the block diagram discussed in the last section, we have implemented Block C4 and Block GC3 decoders with logic synthesis tools in a general-purpose 90 nm bulk-CMOS technology. To accurately estimate the speed, power, and area, each of the building blocks has been translated from the hardware description language to the gate level. Table 4 shows the estimate of area, speed, throughput, and power for Block C4 and Block GC3. Comparing with the LZ77 decoder implemented in our previous work<sup>7</sup>, Block C4 decoder uses half of the area, and results in twice as much compression efficiency. Furthermore, the Block GC3 decoder is half the size of Block C4 decoder.

Table 4. Estimated hardware performance comparison of different data path for direct-write maskless lithography systems.

Block	Area ( $\mu\text{m}^2$ )	$T_p$ (ns)	Throughput (output/cycle)	Power (mW)
Golomb	4,845	1.63	1	1.8
HCC	43,135.	1.43	0.71	7.4
Huffman	2,745	0.83	1/codeword+2	1.6
Linear Prediction	2,674	1.06	1	1.1
Address Generator	1,897	0.6	0.94	0.9
Region Decoder	5,965	1.39	1	1.7
Control/Merge	4,166	0.69	1	1.6
Memory	40,080	1.03	1	1.0

Block C4	Single decoder	100,665	1.43	0.71	24.6
	Total (200)	20,254,592	1.43	0.71	6.375 (W)
Block GC3	Single decoder	62,375	1.63	0.94	19.1
	Total (186)	11,550,960	1.63	0.94	5.192 (W)
Direct-write		--	--	--	10.8 (W)

Table 4 also shows that the critical path for Block C4 is in the HCC block, whereas for Block GC3, the critical path is in the Golomb run-length decoder. This timing analysis indicates that the single Block C4 decoder can operate at 700MHz clock rate, while Block GC3 can only run at 600MHz.

The throughput of the decoder is summarized in Table 4. The throughput is estimated by multiplying the latency for each block by its usage probability. The usage probability is determined by analyzing the encoder statistics of the test layouts. Although the latency of HCC in Block C4 has been smoothed out by applying parallel decoding, there are still some inevitable stall periods in HCC block, resulting in a throughput of 71% of the peak. In contrast, Block GC3 only has a few stalls in the predict/copy segment transition caused by the Address Generator. The throughput of Block GC3 is around 94% of the peak. Combining the clock rate, throughput, and the five-bit output pixel value we compute the output rate of Block C4 and Block GC3 decoders to be 2.48 Gb/s and 2.7 Gb/s respectively for a 1024×1024 image. As a result, 200 Block C4 decoders or 186 Block GC3 decoders are needed to achieve 500 Gb/s output rate, which corresponds to 3 wafer layers per hour. To be competitive with today's optical mask lithography systems which generate one wafer layer per minute, about 5000 decoders are needed to run in parallel.

Table 4 also shows the power consumption of different maskless lithography datapath approaches using gate-level simulations of Block C4 and Block GC3 decoders. As for the direct-write technique, it is possible to apply 80 high-speed I/O pins operating at 6.4 Gb/s to achieve 500 Gb/s data rate without data compression<sup>6</sup>. However, such a method would result in the total power of the writer to be 10.8 W. By applying Block C4 and Block GC3 to the data, the power consumption of the writer chip is substantially reduced. The decrease in the input data rate proportionally decreases the I/O power, thus with the average compression rate higher than 10, as the I/O power is reduced to less than 1W. As shown in Table 4, Block C4 and Block GC3 achieve 41% and 51% power reduction respectively as compared to the direct-write

technique at 500 Gb/s output rate. As compared to Block C4 decoder, Block GC3 decoder achieves 42% area reduction and 18% power reduction, making Block GC3 an attractive option to be implemented in practical maskless lithography systems.

## 7. SUMMARY AND FUTURE WORK

In this paper, we have discussed two variations of C4 to reduce its complexity overhead in both encoding and decoding processes. Block C4 can solve the encoding latency issue by changing the segmentation algorithm into a prediction-based scheme, reducing the encoding time by two orders of magnitude. Block GC3, which replaces HCC by Golomb run-length code for pixel error location coding, can further reduce the hardware decoder overhead of Block C4 by 42% in area and 18% in power.

With scaling of minimum features, the resolution enhancement techniques, e.g. proximity correction, are expected to significantly affect the mask layouts. These techniques add more complex features to the layout, affecting its Manhattan structure. For example, more complex corners will result in more prediction errors in the C4 algorithms, which will affect the compression efficiency. However, the impact will be less severe for dense layouts, where the corrected patterns are repetitive as the original shapes and can be compressed by applying the copying technique. The exact compression efficiency has to be derived by testing the actual enhanced layouts.

In addition, the C4 algorithm can be used to compress rasterized mask layouts for pixel-based mask writers. The compressed files can be stored in the mass storage, and decompressed on-the-fly in software as needed by the mask writer. This flow would require the C4 algorithm to be implemented as a plug-in software and integrated into commercial CAD tools.

We plan to fabricate the Block GC3 decoders in the near future. Subsequently, the integration of decoder and writer chip poses new challenges. One of them is the input balancing problem, where the input data of different decoders are transmitted from common input pins at constant rate from the storage device to the processor board. In such a case, the size of the on-board memory and the access mechanism has to be carefully designed. Also, another important topic to investigate is the mixed signal processing problem from the digital memory to the D/A converters.

## **ACKNOWLEDGEMENTS**

This research was conducted under the Research Network for Advanced Lithography, supported jointly by the Semiconductor Research Corporation (2005-OC-460) and the Defense Advanced Research Project Agency (W911NF-04-1-0304). We would also like to acknowledge Brian Richards of U.C. Berkeley for his invaluable input on hardware design implementation.

## **REFERENCES**

1. V. Dai and A. Zakhor, "Complexity Reduction for C4 Compression for Implementation in Maskless Lithography Datapath," Proc. of the SPIE, 5751(1), pp. 385-400, 2005.
2. V. Dai and A. Zakhor, "Advanced Low-complexity Compression for Maskless Lithography Data," Proc. of the SPIE, 5374 (1), pp. 610-618, 2004.
3. V. Dai and A. Zakhor, "Binary Combinatorial Coding," Proc. of the Data Compression Conference 2003, pp. 420, 2003.
4. V. Dai and A. Zakhor, "Lossless Compression Techniques for Maskless Lithography Data," Proc. of the SPIE, 4688, pp. 583-594, 2002.
5. V. Dai, A. Zakhor, "Lossless Layout Compression for Maskless Lithography," Proc. of the SPIE, 3997, pp. 467-77, 2000.
6. K. Chang, S. Pamarti, K. Kaviani, E. Alon, X. Shi, T.J. Chin, J. Shen, G. Yip, C. Madden, R. Schmitt, C. Yuan, F. Assaderaghi, and M. Horowitz, "Clocking and Circuit Design for A Parallel I/O on A First-Generation CELL Processor," in IEEE International Solid-State Circuit Conference, 2005.
7. B. Nikolić, B. Wild, V. Dai, Y. Shroff, B. Warlick, A. Zakhor, and W. G. Oldham, "Layout Decompression Chip for Maskless Lithography," Proc. of the SPIE, 5374 (1), pp. 1092-1099, 2004.
8. S. W. Golomb, "Run-length Encodings," IEEE Trans. on Information Theory, IT-12 (3), pp. 399-401, 1966.
9. M.-T. Sun, "VLSI Architecture and Implementation of A High-Speed Entropy Decoder," IEEE International Symposium on Circuits and Systems, pp. 200 – 203, 1991

10. M. J. Weinberger, G. Seroussi, and G. Sapiro, “The LOCO-I lossless image compression algorithm: principles and standardization into JPEG-LS,” IEEE Trans. on Image Processing, 9 (8), pp.1309-1324, 2000.
11. J. Ziv, and A. Lempel, “A universal algorithm for sequential data compression”, IEEE Trans. on Information Theory, IT-23 (3), pp. 337-43, 1977.
12. ITRS, “International Technology Roadmap for Semiconductors 2005 Edition – Lithography,” <http://www.itrs.net>.